To be published in The Astrophysical Journal Letters
Preprint typeset using LaTeX style emulateapj v. 11/10/09

SIGNATURES OF DARK MATTER BURNING IN NUCLEAR STAR CLUSTERS

Jordi Casanellas[1,3], Ilídio Lopes[1,2,4]

To be published in The Astrophysical Journal Letters

ABSTRACT

In order to characterize how dark matter (DM) annihilation inside stars changes the aspect of a stellar cluster we computed the evolution until the ignition of the He burning of stars from 0.7 $M_\odot$ to 3.5 $M_\odot$ within halos of DM with different characteristics. We found that, when a cluster is surrounded by a dense DM halo, the positions of the cluster' stars in the H-R diagram have a brighter and hotter turn-off point than in the classical scenario without DM, therefore giving the cluster a younger appearance. The high DM densities required to produce these effects are expected only in very specific locations, such as near the center of our Galaxy. In particular, if DM is formed by the 8 GeV WIMPs recently invoked to reconcile the results from direct detection experiments, then this signature is predicted for halos of DM with a density $\rho_\chi = 3 \cdot 10^5$ GeV cm^{-3}. A DM density gradient inside the stellar cluster would result in a broader main sequence, turn-off and red giant branch regions. Moreover, we found that for very high DM halo densities the bottom of the isochrones in the H-R diagram rises to higher luminosities, leading to a characteristic signature on the stellar cluster. We argue that this signature could be used to indirectly probe the presence of DM particles in the location of a cluster.

Subject headings: dark matter - Galaxies: star clusters - Galaxy: center - Hertzsprung-Russell diagrams - Stars: fundamental parameters

1. INTRODUCTION

An unambiguous discovery of the particle nature of dark matter (DM) would have to come simultaneously from a variety of experiments and observations (Bertone 2010). Positive results from direct detection experiments (Cerdeño & Green 2010; Pato et al. 2010) and the hypothetical evidence of the existence of new particles from colliders (Bertone et al. 2010) must be complemented by indirect methods, such as the detection of DM annihilation products (Trotta et al. 2009; Scott et al. 2010; Bernal & Palomares-Ruiz 2010) or the observation of a peculiar signature in the solar neutrinos attributed to the effect of captured DM particles (Taoso et al. 2010; Lopes & Silk 2010a).

In the last years many works studied the effects of WIMP DM on stellar evolution (Spolyar et al. 2008; Bertone & Fairbairn 2008; Iocco 2008; Yoon et al. 2008; Taoso et al. 2008; Ripamonti et al. 2010; Gondolo et al. 2010; Sivertsson & Gondolo 2010; de Lavallaz & Fairbairn 2010; Zackrisson et al. 2010; Kouvaris & Tinyakov 2010; Yuan et al. 2011) as a promising complementary way to investigate the nature of DM. Remarkably, it has also been argued that the seismological analysis of the stellar oscillations could be used to detect the signature of captured DM particles in the Sun (Cumberbatch et al. 2010; Lopes & Silk 2010b) and in other sun-like stars in environments with very high DM densities (Casanellas & Lopes 2011). All these studies require DM particles to interact with a non-zero nuclear scattering cross section.

[1] Centro Multidisciplinar de Astrofísica, Instituto Superior Técnico, Av. Rovisco Pais, 1049-001 Lisboa, Portugal
[2] Departamento de Física, Universidade de Évora, Colégio Luis António Verney, 7002-554 Évora - Portugal
[3] E-mail: jordicasanellas@ist.utl.pt
[4] E-mail: ilidio.lopes@ist.utl.pt

In this work we are interested in the global behavior of a large group of stars instead of being concerned with the influence of DM on a single star, whose observation would require a higher precision. We address the question of how a dense halo of DM particles changes the properties of an embedded cluster of stars. As we will show, the annihilation of captured DM particles inside the stars leaves strong signatures in the stellar cluster when compared with a classical cluster without DM. The high DM densities required to produce measurable effects on the cluster restrict our study to the nuclear star clusters, present in the centers of galaxies, where the highest DM densities are expected. Our description of the cluster isochrones provides an indirect way to probe the presence of DM particles in the location of the cluster, as the signatures we describe here are difficult to attribute to other processes.

This letter is organized as follows: the physics beyond the stellar models and the capture and annihilation of DM particles is briefly described in Section 2; the effects of DM on stellar evolution are characterized in Section 3; in Section 4 the properties of a cluster embedded in a dense DM halo are compared with those of a classical cluster; finally, we conclude in Section 5 with a brief discussion of our results.

2. STELLAR AND DARK MATTER PHYSICS

To compute our stellar models we used the stellar evolution code CESAM (Morel 1997). This code has an up-to-date and very refined microscopic physics, tested against helioseismic data (Turck-Chieze & Lopes 1993; Turck-Chièze et al. 2010). Our stellar models were evolved from the zero age main sequence (ZAMS) (although some of them were also evolved from the pre-main sequence phase to check that both approaches led to similar results), at constant mass, with a metallicity $Z = 0.019$ and an initial helium mass fraction $Y = 0.273$

similar to the solar ones. The initial abundance of the other elements was set equal to the solar composition. The mixing-length parameter was set by calibrating a solar model with an accuracy of 10^{-5} on the solar radius and luminosity. The performance of our code in the range of masses (0.7 $M_\odot$ to 3.5 $M_\odot$) and evolutionary stages studied in this work was successfully tested by comparing our computed isochrones with those of Girardi et al. (2000).

The stars computed in this work are embedded in a dense halo of DM. To account for the impact of the DM particles on the stars we considered that some of the DM particles that populate the halo are gravitationally captured by the stars and accumulate in their interior. The number of captured DM particles was computed using the integral expression of Gould (1987), as implemented in Gondolo et al. (2004). Note that, for the capture process to be efficient, the DM particles are assumed to have a non-negligible scattering cross section with baryons σ_χ, which we chose to be smaller than the present limits from direct detection experiments: $\sigma_{\chi,SI} = 10^{-44}$ cm^2 (Ahmed et al. 2010) and $\sigma_{\chi,SD} = 10^{-38}$ cm^2 (Behnke et al. 2011) for a WIMP with a mass of 100 GeV. For these values of σ_χ, the spin-dependent (SD) interactions with hydrogen atoms always dominate over the spin-independent (SI) ones with other stellar isotopes.

In the capture rate (C_χ) calculation we assumed a stellar velocity $v_\star = 220$ km s^{-1} and a Maxwellian DM velocity distribution with a dispersion $\bar{v_\chi} = 270$ km s^{-1}. These values apply for the solar case, but are certainly inaccurate for a nuclear cluster. For instance, stars with velocities as high as 400 km s^{-1} are observed near the Galactic center (GC) (Lu et al. 2009). In this case the capture rate would be reduced by a factor of 6 (for a more thorough analysis of how C_χ varies for different stellar and DM characteristics see Lopes, Casanellas & Eugénio (2011)). At the same time, it is complex to model the DM velocity distribution in the GC, as the motion of the DM particles is strongly influenced by the gravitational potential of the stars and the central black hole. Interestingly, Scott et al. (2009) tested other DM velocity distributions with the aim of grasping the possible variations on C_χ. When a non-Gaussian distribution (designed to fit a N-body simulation of a Milky Way-size DM halo) was implemented, the capture rate was boosted by a factor of 3-5. On the other hand, the same authors found that the truncation of the isothermal distribution at the local escape velocity reduces C_χ by a factor of 2. The same order of uncertainty on C_χ is expected in the cases presented in the present work.

After some scatterings, the DM particles sink to the core of the star and rapidly thermalize with stellar matter. The number of DM particles in the stellar core increases until their self-annihilation rate balances the capture rate. This equilibrium is reached in a time scale below 10^4 yr for all cases studied here. Thus, the annihilation of DM particles provides a new source of energy which contributes to the total luminosity of the star according to (Salati & Silk 1989):

$$L_\chi = f_\chi \, m_\chi \, C_\chi \, , \qquad (1)$$

where m_χ is the mass of the DM particles, and $f_\chi = 2/3$ to take into account that one third of the energy may escape the star in the form of neutrinos (Iocco et al. 2008). This energy is injected to the stellar models following the thermal distribution of the DM particles, which characteristic radius is below 2% and 7% of the stellar radius for $m_\chi = 100$ GeV and 8 GeV respectively. The total input of energy from DM annihilation, and thus also its impact on stellar evolution, will depend mainly on the product $\rho_\chi \sigma_\chi$.

3. STELLAR EVOLUTION WITHIN DENSE DM HALOS

The hydrostatic equilibrium (the balance between pressure and gravity) achieved by a star within a dense DM halo differs from the one reached in the classical picture due to the new source of energy added to the classical thermonuclear energy sources. This fact leads to three main consequences that will influence the characteristics of the whole cluster:

1. *Slowing of the evolutionary speed*: The central temperature of stars that evolve within dense DM halos is lower than that of classical stars due to their negative heat capacity. Another simple way to understand this is to imagine a forming star in the pre-main sequence. The cloud of gas that forms the proto-star shrinks, increasing its central temperature until the gravitational collapse is balanced by the thermonuclear reactions; if another source of energy helps to compensate gravity, the hydrostatic equilibrium is reached earlier, when the central temperature is lower. Therefore, stars within dense DM halos burn hydrogen at a lower rate, slowing down their evolution through later phases. For example, a star of 1 $M_\odot$ will spend more than 20 Gyr in the main sequence (MS) if it evolves in a DM halo of density $\rho_\chi = 2{\cdot}10^9$ GeV cm^{-3} (assuming $\sigma_{\chi,SD} = 10^{-38}$ cm^2, although other values of ρ_χ and $\sigma_{\chi,SD}$ can be considered, leading to the same effects as long as the product $\rho_\chi \sigma_\chi$ is kept constant). This is a significant difference from the classical picture, in which a star as the Sun is expected to exhaust its hydrogen core in less than 10 Gyr. As shown in earlier works (Salati & Silk 1989), the more massive the star is, the less it is affected by WIMP annihilation. Considering the same DM halo of the previous example, a star of 3 $M_\odot$ won't be affected.

2. *Different paths on the H-R diagram*: Since DM burning accounts for at least one third of the total energy, the balance will be reached with a larger radius and a lower effective temperature than in the classical picture (Fairbairn et al. 2008). Therefore, stars that evolve in dense DM halos follow slightly different paths in the H-R diagram. We found that, in addition to the different paths followed during the MS, which was already reported in previous works (Casanellas & Lopes 2009), stars follow brighter tracks during the red giant branch (RGB). This feature is illustrated in Figure 1. Even if the difference in the paths is remarkable, its effect on the cluster is small compared with the slowing of the evolutionary speed.

3. *Stationary states*: For extremely high DM densities, stars are powered only by the energy from DM annihilation. Whether the star was formed in this environment or arrived there a posteriori, it will reach a state of equilibrium in the Hyashi track, far from the MS where most stars are found (Casanellas & Lopes 2009). In this case

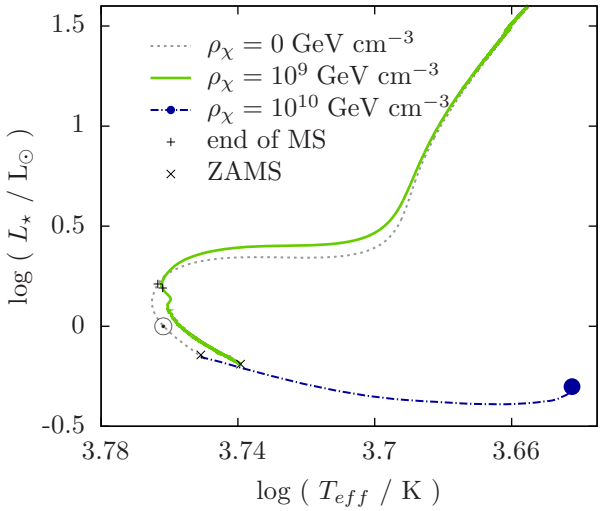

FIG. 1.— Tracks on the H-R diagram of stars of 1 $M_\odot$ that evolved in halos with different DM densities. The blue point indicates a stationary state reached by a star only powered by DM burning. We considered DM particles with a mass $m_\chi = 100$ GeV and a spin-dependent scattering cross section with protons $\sigma_{\chi,SD} = 10^{-38}$ cm^2.

the star is fully convective and remains in the same position in the H-R diagram as long as there are DM particles to be captured in the halo (an illustrative example is shown in Figure 1).

4. GLOBAL STRUCTURE OF A STELLAR CLUSTER WITHIN A DENSE DM HALO

It is naturally expected then, that stellar clusters are affected by DM halos, since their basic constituents, namely stars, are themselves affected. The main reason is the fact that stars with lower masses evolve slower in dense DM halos. This effect is not noticeable for young clusters since in these clusters low-mass stars are still in the MS and the more massive ones, which are evolving through the RGB, are not affected by the presence of DM. However, in old clusters the RGB may be populated by stars that evolved slower, consequently making the cluster look younger than its real age. Moreover, the fact that low-mass stars within dense DM halos follow brighter paths in the RGB than classical stars contributes to amplify this effect.

In order to distinctly illustrate the younger appearance of a cluster when embedded in a dense DM halo, we computed the isochrones (the track drawn by the positions in the H-R diagram of all stars with different masses at a given age) of stellar clusters in different situations. Figure 2 shows the isochrones we obtained for a cluster evolving in a halo of DM with a density $\rho_\chi = 10^9$ GeV cm^{-3} (continuous lines) together with those obtained without the influence of DM (dashed lines). When the isochrones of ≥ 1000 Myr in both situations are compared, we see that indeed the cluster within a dense DM halo looks younger, with a brighter and hotter turn-off point and a brighter RGB. In this case the turn-off and RGB are populated by more massive stars than in the classical scenario, because they took longer to burn out their hydrogen core and to leave the MS. It is almost impossible to distinguish both clusters at ages ≤ 500 Myr.

When even higher DM densities are considered (or, equivalently, larger WIMP-on-nucleon scattering cross

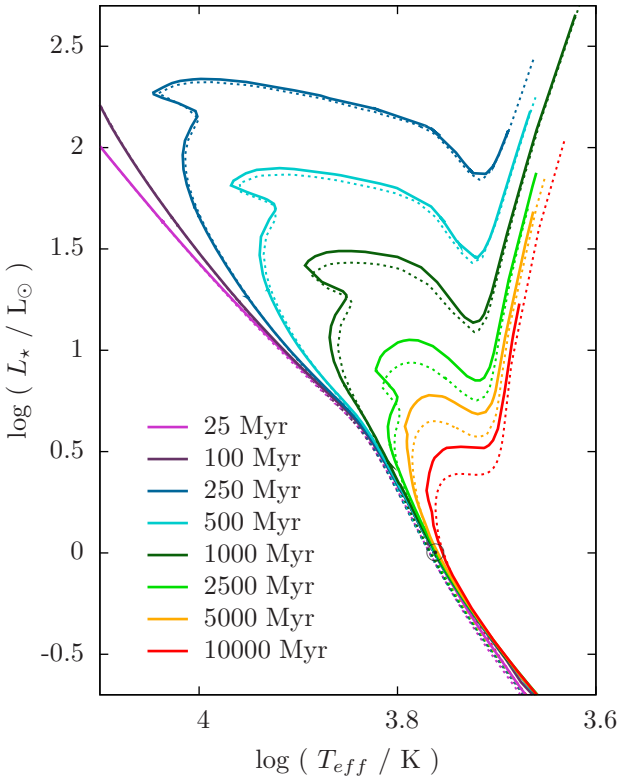

FIG. 2.— Isochrones for a cluster of stars with masses between 0.7 $M_\odot$-3.5 $M_\odot$ that evolved in a halo of DM with a density $\rho_\chi = 10^9$ GeV cm^{-3} (continuous lines) and for the same cluster in the classical scenario without DM (dashed lines). We considered DM particles with a mass $m_\chi = 100$ GeV and a spin-dependent scattering cross section with protons $\sigma_{\chi,SD} = 10^{-38}$ cm^2.

sections) the characteristics of the cluster change dramatically. In addition to the previously described effect (which will now be visible for younger clusters, because at higher DM densities more massive stars will be affected), another strong signature of the presence of DM in the halo arises when looking at the position of stars with lower masses. These stars, which are mostly fueled by the energy from DM annihilation, go back in the Hyashi track and reach positions in the H-R diagram which were normally occupied only by forming stars in their way to the MS. Consequently, the bottom of the isochrones, corresponding to the lower mass stars, rises to higher luminosities, giving the cluster a very characteristic appearance. This peculiar signature is a strong indication of the presence of high concentrations of DM in a stellar cluster.

This strong signature is illustrated in Figure 3, where the isochrones of a stellar cluster surrounded by a halo of DM with a density $\rho_\chi = 10^{10}$ GeV cm^{-3} are plotted. The main characteristic signature of the presence of DM is the fact that the bottom of all isochrones is more than 3 times brighter than the classical isochrones. In addition, the effect of a brighter and hotter turn-off point is now more pronounced and appreciable in clusters as young as 250 Myr.

We have also considered the hypothetical scenario in which DM is formed by the low-mass WIMPs invoked to reconcile the results of DAMA with the negative results of other direct detection experiments (Savage et al. 2009). As shown in Figure 4, if such WIMPs form most

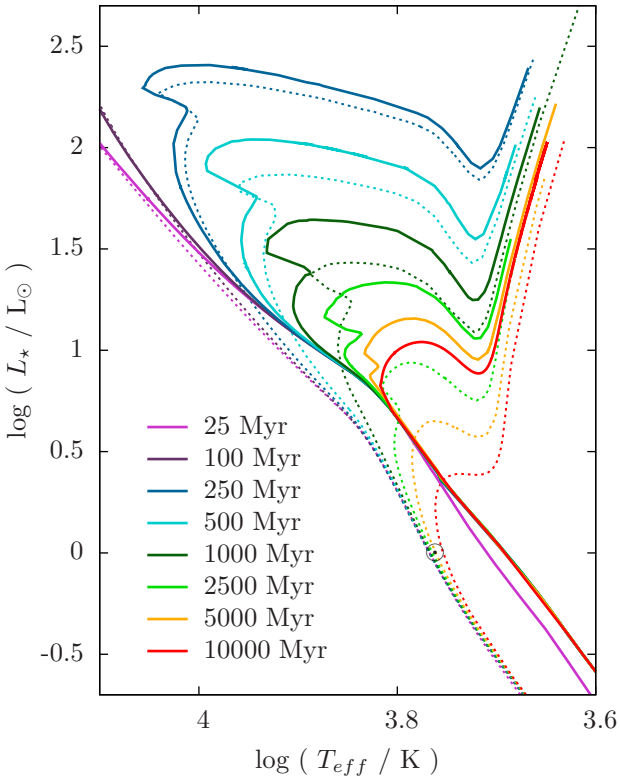

FIG. 3.— Isochrones for a cluster of stars with masses between 0.7 $M_\odot$-3.5 $M_\odot$ that evolved in a halo of DM with a density $\rho_\chi = 10^{10}$ GeV cm^{-3} (continuous lines) and for the same cluster in the classical scenario without DM (dashed lines). The post-MS segment of the 10 Gyr isochrone is a conservative estimation (a lower limit on luminosity) of the true isochrone. We considered DM particles with a mass $m_\chi = 100$ GeV and a spin-dependent scattering cross section with protons $\sigma_{\chi,SD} = 10^{-38}$ cm^2.

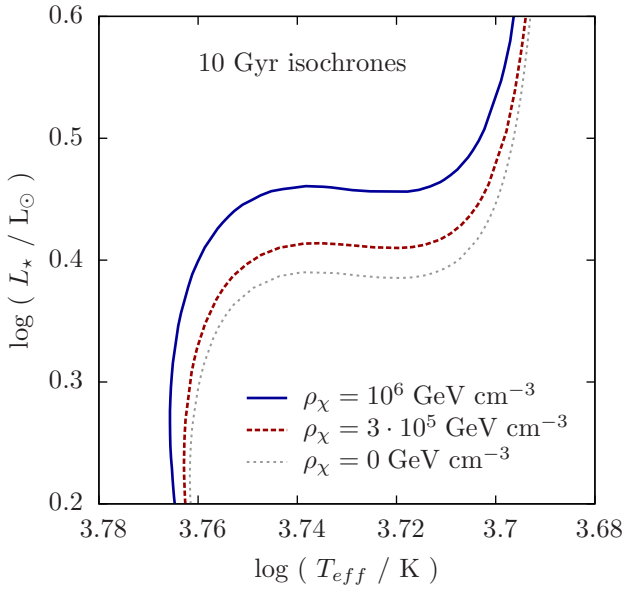

FIG. 4.— Isochrones of 10 Gyr for clusters of stars that evolved in halos of DM with different densities. We considered DM particles with the particular characteristics that fit DAMA observations and constraints from direct detection experiments: a mass $m_\chi = 8$ GeV and a spin-dependent scattering cross section with protons $\sigma_{\chi,SD} = 10^{-36}$ cm^2.

of the DM then the DM density needed to have signatures on a stellar cluster would be as low as $3 \cdot 10^5$ GeV cm^{-3}. Both the low mass of these WIMPs ($m_\chi = 8$ GeV) and especially their large SD scattering cross section with protons ($\sigma_{\chi,SD} = 10^{-36}$ cm^2) contribute to producing effects on the stellar cluster at lower DM halo densities.

5. DISCUSSION AND CONCLUSIONS

We have shown that a cluster of stars that evolves in a dense halo of DM shows strong signatures in its appearance due to the self-annihilation of captured DM particles in the interior of stars. In comparison to the classical case, the cluster within a dense DM halo looks younger than its true age, due to the slower evolution of the stars when these are partially powered by DM annihilation. This is visible only for old clusters (e.g. for clusters older than 1 Gyr within a DM halo of density $\rho_\chi = 10^9$ GeV cm^{-3}), because their RGB is populated by low-mass stars, which are the type of stars most affected by DM.

Our work focuses on environments with very high DM densities, which may be present only in specific locations, such as near the centers of galaxies (Gondolo & Silk 1999). In particular, considering an adiabatically contracted DM profile (Bertone & Merritt 2005), the DM densities discussed here may be found at the following distances from the GC: $\rho_\chi = 3 \times 10^5$ GeV cm^{-3} at $r_{GC} \approx 1$ pc and $\rho_\chi = 10^{10}$ GeV cm^{-3} at $r_{GC} \approx 0.01$ pc. The shape of the central profiles of galactic DM halos is still a topic of discussion (de Blok 2010): while simulations predict the existence of cusps, observations favor constant-density DM cores.

Our results indicate that the age of a cluster may be underestimated if embedded in a dense DM halo, which goes towards solving the "paradox of youth" in the center of the Milky Way, a possibility that was first suggested by Moskalenko & Wai (2007) in the context of compact stars. However, there are many astrophysical uncertainties, such as the velocities of stars and DM particles, that may change the rate at which stars capture DM particles and therefore change the overall influence of DM on a cluster. Although our results do not explain the depletion of giants observed in the nuclear central cluster of the Milky Way (Do et al. 2009; Buchholz et al. 2009; Bartko et al. 2010) they show that the influence of DM on stellar evolution must be taken into account when studying nuclear clusters.

A DM halo density gradient inside the stellar cluster would result in a broader MS, turn-off and RGB regions. This effect is usually attributed to photometric errors, variable reddening (Carraro et al. 2002), extended star formation (Twarog et al. 2011) and binaries (Zhao & Bailyn 2005). In the case of nuclear star clusters it could also be associated with the annihilation of DM particles inside the stars, given that within the typical size of nuclear clusters the DM density is expected to vary several orders of magnitude depending on the proximity of the galactic center.

For stellar clusters embedded in halos with extremely high DM densities we found an additional very strong signature: the bottom of the computed isochrones in the H-R diagram rises to higher luminosities because the low-mass stars, powered only with energy from DM annihilation, inflate and become fully convective. As this signature is hardly explained by other processes, we argue that this could be an indirect way to probe the presence

of DM particles in the location of a cluster of stars.

We are grateful to the authors of DarkSUSY, from which some of the publicly available routines were adapted, and CESAM, as well as to the anonymous referee for a careful review. This work was supported by grants from FCT-MCTES (SFRH/BD/44321/2008) and Fundação Calouste Gulbenkian.

REFERENCES

Ahmed, Z. et al. (CDMS II Collaboration) 2010, Science, 327, 1619-, arXiv:0912.3592
Bartko, H. et al. 2010, ApJ, 708, 834, arXiv:0908.2177
Behnke, E. et al. (COUPP Collaboration) 2011, Physical Review Letters, 106, 021303, arXiv:1008.3518
Bernal, N. & Palomares-Ruiz, S. 2010, arXiv:1006.0477
Bertone, G. 2010, Nature, 468, 389, arXiv:1011.3532
Bertone, G., Cerdeno, D. G., Fornasa, M., de Austri, R. R., & Trotta, R. 2010, Phys. Rev., D82, 055008, arXiv:1005.4280
Bertone, G. & Fairbairn, M. 2008, Phys. Rev. D, 77, 043515, arXiv:0709.1485
Bertone, G. & Merritt, D. 2005, Modern Physics Letters A, 20, 1021, arXiv:astro-ph/0504422
Buchholz, R. M., Schödel, R., & Eckart, A. 2009, A&A, 499, 483, arXiv:0903.2135
Carraro, G., Girardi, L., & Marigo, P. 2002, MNRAS, 332, 705, arXiv:astro-ph/0202018
Casanellas, J. & Lopes, I. 2009, ApJ, 705, 135, arXiv:0909.1971
Casanellas, J. & Lopes, I. 2011, MNRAS, 410, 535, arXiv:1008.0646
Cerdeño, D. G. & Green, A. M. Direct detection of WIMPs, ed. Bertone, G. (Cambridge University Press), 347–+, arXiv:1002.1912
Cumberbatch, D. T., Guzik, J., Silk, J., Watson, L. S., & West, S. M. 2010, Phys. Rev., D82, 103503, arXiv:1005.5102
de Blok, W. J. G. 2010, Advances in Astronomy, vol. 2010, 789293, doi:10.1155/2010/789293, arXiv:0910.3538
de Lavallaz, A. & Fairbairn, M. 2010, Phys. Rev. D, 81, 123521, arXiv:1004.0629
Do, T., Ghez, A. M., Morris, M. R., Lu, J. R., Matthews, K., Yelda, S., & Larkin, J. 2009, ApJ, 703, 1323, arXiv:0908.0311
Fairbairn, M., Scott, P., & Edsjö, J. 2008, Phys. Rev. D, 77, 047301, arXiv:0710.3396
Girardi, L., Bressan, A., Bertelli, G., & Chiosi, C. 2000, A&AS, 141, 371, arXiv:astro-ph/9910164
Gondolo, P., Edsjö, J., Ullio, P., Bergström, L., Schelke, M., & Baltz, E. A. 2004, JCAP, 7, 008, arXiv:astro-ph/0406204
Gondolo, P., Huh, J., Do Kim, H., & Scopel, S. 2010, JCAP, 7, 26, arXiv:1004.1258
Gondolo, P. & Silk, J. 1999, Phys. Rev. Lett., 83, 1719, arXiv:astro-ph/9906391
Gould, A. 1987, ApJ, 321, 571
Iocco, F. 2008, ApJ, 677, L1, arXiv:0802.0941
Iocco, F., Bressan, A., Ripamonti, E., Schneider, R., Ferrara, A., & Marigo, P. 2008, MNRAS, 390, 1655, arXiv:0805.4016
Kouvaris, C. & Tinyakov, P. 2011, Phys. Rev. D, 83, 083512, arXiv:1012.2039
Lopes, I., Casanellas, J. & Eugénio, D. 2011, Phys. Rev. D, 83, 063521, arXiv:1102.2907
Lopes, I. & Silk, J. 2010a, Science, 330, 462
Lopes, I. & Silk, J. 2010b, ApJ, 722, L95, arXiv:1009.5122
Lu, J. R. m*-+al. 2009, ApJ, 690, 1463, arXiv:0808.3818
Morel, P. 1997, A&As, 124, 597,
Moskalenko, I. V. & Wai, L. L. 2007, ApJ, 659, L29, arXiv:astro-ph/0702654
Pato, M., Baudis, L., Bertone, G., Ruiz de Austri, R., Strigari, L. E., & Trotta, R. 2011, Phys. Rev. D, 83, 083505, arXiv:1012.3458
Ripamonti, E., Iocco, F., Ferrara, A., Schneider, R., Bressan, A., & Marigo, P. 2010, MNRAS, 406, 2605, arXiv:1003.0676
Salati, P. & Silk, J. 1989, ApJ, 338, 24
Savage, C., Gelmini, G., Gondolo, P., & Freese, K. 2009, JCAP, 4, 010, arXiv:0808.3607
Scott, P., Conrad, J., Edsjö, J., Bergström, L., Farnier, C., & Akrami, Y. 2010, JCAP, 1, 31, arXiv:0909.3300
Scott, P., Fairbairn, M., & Edsjö, J. 2009, MNRAS, 394, 82, arXiv:0809.1871
Sivertsson, S. & Gondolo, P. 2011, ApJ, 729, 51, arXiv:1006.0025
Spolyar, D., Freese, K., & Gondolo, P. 2008, Phys. Rev. Lett., 100, 051101, arXiv:0705.0521
Taoso, M., Bertone, G., Meynet, G., & Ekström, S. 2008, Phys. Rev. D, 78, 123510, arXiv:0806.2681
Taoso, M., Iocco, F., Meynet, G., Bertone, G., & Eggenberger, P. 2010, Phys. Rev. D, 82, 083509, arXiv:1005.5711
Trotta, R., Ruiz de Austri, R., & Pérez de los Heros, C. 2009, JCAP, 8, 34, arXiv:0906.0366
Turck-Chieze, S. & Lopes, I. 1993, ApJ, 408, 347,
Turck-Chièze, S., Palacios, A., Marques, J. P., & Nghiem, P. A. P. 2010, ApJ, 715, 1539, arXiv:1004.1657
Twarog, B. A., Carraro, G., & Anthony-Twarog, B. J. 2011, ApJ, 727, L7+, arXiv:1011.5138
Yoon, S. C., Iocco, F., & Akiyama, S. 2008, ApJ, 688, L1, arXiv:0806.2662
Yuan, Q., Yue, B., Zhang, B., & Chen, X. 2011, JCAP, 4, 020, arXiv:1104.1233
Zackrisson, E. et al. 2010, ApJ, 717, 257, arXiv:1002.3368
Zhao, B. & Bailyn, C. D. 2005, AJ, 129, 1934,

APPENDIX

ISOCHRONE TABLES

In Table 1 is shown a summary of the data used in Figures 2 and 3, which corresponds to the isochrones of a classical stellar cluster and of stellar clusters embedded in halos of DM particles with densities $\rho_\chi = 10^9$ GeV cm^{-3} and $\rho_\chi = 10^{10}$ GeV cm^{-3}. The mass of the stars ranges from 0.7 to 3.5 $M_\odot$ and their metallicity is Z=0.019. Our results do not rely on any specific initial mass function (IMF), i.e. any IMF could be used along with the table to obtain the relative number of stars in different sections of the isochrones.

TABLE 1 Isochrones of a stellar cluster embedded in halos of DM particles with different DM densities. The DM particles are assumed to have a mass of 100 GeV and a spin-dependent scattering cross section with protons $\sigma_{\chi,SD} = 10^{-38}$ cm^2.

ρ_χ (GeV cm^{-3})	*Age* (Myr)	$M(M_\odot)$	$\log(T_{eff}$ / K)	$\log(L_\star$ / $L_\odot$)
0	25	0.75000	3.67148	-0.73140
0	25	0.75000	3.67148	-0.73140
0	25	0.85000	3.70861	-0.47804
0	25	0.90000	3.72415	-0.36338
0	25	0.95000	3.73803	-0.25484
0	25	1.00000	3.75052	-0.15104
0	25	1.05000	3.76194	-0.05041
0	25	1.10000	3.77265	0.04843
0	25	1.20000	3.79237	0.23570
0	25	1.30000	3.81074	0.40377
0	25	1.40000	3.82962	0.55440
0	25	1.50000	3.85267	0.68920
0	25	1.60000	3.87884	0.81074
0	25	1.70000	3.90249	0.92201
0	25	1.80000	3.92363	1.02498
0	25	1.90000	3.94274	1.12120
0	25	2.00000	3.96023	1.21166
0	25	2.10000	3.97637	1.29708
0	25	2.20000	3.99138	1.37803
0	25	2.30000	4.00538	1.45504
0	25	2.40000	4.01853	1.52842
0	25	2.50000	4.03089	1.59858
0	25	2.60000	4.04258	1.66576
0	25	2.70000	4.05366	1.73024
0	25	2.80000	4.06423	1.79230
0	25	2.90000	4.07430	1.85203
0	25	3.00000	4.08393	1.90969
0	25	3.10000	4.09316	1.96535
0	25	3.20000	4.10202	2.01921
0	100	0.75000	3.66983	-0.72340
0	100	0.85000	3.70742	-0.47299
0	100	0.90000	3.72360	-0.35737
0	100	0.95000	3.73832	-0.24661
0	100	1.00000	3.75162	-0.14020
0	100	1.05000	3.76357	-0.03808
0	100	1.10000	3.77436	0.05996
0	100	1.20000	3.79377	0.24417
0	100	1.30000	3.81202	0.41114
0	100	1.40000	3.83076	0.56072
0	100	1.50000	3.85351	0.69513
0	100	1.60000	3.87902	0.81715
0	100	1.70000	3.90196	0.92923
0	100	1.80000	3.92235	1.03330
0	100	1.90000	3.94060	1.13064
0	100	2.00000	3.95705	1.22230
0	100	2.10000	3.97206	1.30915
0	100	2.20000	3.98581	1.39169
0	100	2.30000	3.99862	1.47068
0	100	2.40000	4.01057	1.54636
0	100	2.50000	4.02180	1.61927
0	100	2.60000	4.03235	1.68947
0	100	2.70000	4.04228	1.75733
0	100	2.80000	4.05165	1.82309
0	100	2.90000	4.06046	1.88690
0	100	3.10000	4.07652	2.00952
0	100	3.30000	4.09055	2.12621
0	100	3.50000	4.10250	2.23821
0	250	0.75000	3.66912	-0.72153
0	250	0.85000	3.70739	-0.46915

Continued on next page

TABLE 1 – continued from previous page

ρ_χ (GeV cm^{-3})	*Age* (Myr)	$M(\mathrm{M}_\odot)$	$\log(T_{eff}$ / K)	$\log(L_\star$ / $\mathrm{L}_\odot$)
0	250	0.90000	3.72389	-0.35231
0	250	0.95000	3.73879	-0.24068
0	250	1.00000	3.75213	-0.13382
0	250	1.10000	3.77490	0.06741
0	250	1.20000	3.79430	0.25283
0	250	1.30000	3.81246	0.42100
0	250	1.40000	3.83101	0.57182
0	250	1.50000	3.85331	0.70756
0	250	1.60000	3.87778	0.83108
0	250	1.70000	3.89929	0.94477
0	250	1.80000	3.91773	1.05040
0	250	1.90000	3.93384	1.15023
0	250	1.91000	3.93532	1.15989
0	250	2.00000	3.94803	1.24461
0	250	2.10000	3.96078	1.33514
0	250	2.20000	3.97224	1.42220
0	250	2.30000	3.98254	1.50639
0	250	2.40000	3.99160	1.58793
0	250	2.50000	3.99942	1.66736
0	250	2.60000	4.00586	1.74458
0	250	2.70000	4.01069	1.82007
0	250	2.80000	4.01363	1.89408
0	250	2.90000	4.01403	1.96626
0	250	3.00000	4.01103	2.03676
0	250	3.10000	4.00409	2.10587
0	250	3.15000	4.00024	2.14164
0	250	3.20000	4.01325	2.19874
0	250	3.21000	4.04108	2.26802
0	250	3.22000	4.02978	2.29505
0	250	3.23000	4.02127	2.30979
0	250	3.24000	4.00720	2.32118
0	250	3.24500	3.98751	2.32297
0	250	3.25000	3.95206	2.30835
0	250	3.25150	3.93486	2.29574
0	250	3.25350	3.90164	2.26602
0	250	3.25500	3.89325	2.25815
0	250	3.25590	3.87516	2.24086
0	250	3.25600	3.83402	2.18768
0	250	3.25630	3.82425	2.17807
0	250	3.25650	3.81795	2.16721
0	250	3.25680	3.78730	2.12451
0	250	3.25710	3.78140	2.11338
0	250	3.25750	3.77872	2.10775
0	250	3.25800	3.76515	2.07537
0	250	3.25830	3.75982	2.05500
0	250	3.25870	3.74219	1.96290
0	250	3.25900	3.73576	1.92345
0	250	3.25950	3.72738	1.87437
0	250	3.25980	3.71750	1.84125
0	250	3.26000	3.71397	1.84491
0	250	3.26100	3.70422	1.89534
0	250	3.26200	3.69260	2.01970
0	250	3.26300	3.68374	2.13944
0	250	3.26500	3.67265	2.29575
0	250	3.26700	3.66270	2.43925
0	500	0.75000	3.66911	-0.71835
0	500	0.85000	3.70780	-0.46408
0	500	0.90000	3.72443	-0.34634
0	500	0.95000	3.73938	-0.23390
0	500	1.00000	3.75276	-0.12610
0	500	1.10000	3.77554	0.07749
0	500	1.20000	3.79490	0.26571
0	500	1.30000	3.81286	0.43662
0	500	1.40000	3.83086	0.58981
0	500	1.50000	3.85171	0.72776
0	500	1.60000	3.87358	0.85341
0	500	1.70000	3.89155	0.96972
0	500	1.80000	3.90572	1.07833
0	500	1.90000	3.91734	1.18272
0	500	2.00000	3.92637	1.28295
0	500	2.04000	3.92920	1.32207
0	500	2.10000	3.93249	1.37987
0	500	2.20000	3.93491	1.47332
0	500	2.30000	3.93224	1.56312
0	500	2.40000	3.92290	1.64869
0	500	2.46000	3.92378	1.71275

Continued on next page

TABLE 1 – continued from previous page

ρ_χ (GeV cm^{-3})	*Age* (Myr)	$M(\mathrm{M}_\odot)$	$\log(T_{eff}$ / K)	$\log(L_\star$ / $\mathrm{L}_\odot$)
0	500	2.46500	3.92800	1.72412
0	500	2.47000	3.93591	1.74035
0	500	2.47500	3.95797	1.78130
0	500	2.48000	3.95911	1.82439
0	500	2.50000	3.93963	1.86087
0	500	2.51000	3.91183	1.86722
0	500	2.51200	3.90364	1.86503
0	500	2.51400	3.88457	1.85568
0	500	2.51600	3.86064	1.83821
0	500	2.51800	3.82350	1.80095
0	500	2.51900	3.80242	1.77489
0	500	2.52000	3.78050	1.73315
0	500	2.52100	3.76165	1.65732
0	500	2.52200	3.74752	1.55854
0	500	2.52300	3.73554	1.48007
0	500	2.52400	3.72477	1.43067
0	500	2.52500	3.71456	1.45750
0	500	2.52700	3.69870	1.65553
0	500	2.53000	3.68516	1.87425
0	500	2.53500	3.66891	2.12896
0	500	2.53700	3.66378	2.20523
0	500	2.53810	3.66086	2.24817
0	1000	0.75000	3.66966	-0.71245
0	1000	0.85000	3.70876	-0.45537
0	1000	0.90000	3.72551	-0.33606
0	1000	0.95000	3.74054	-0.22176
0	1000	1.00000	3.75396	-0.11176
0	1000	1.10000	3.77672	0.09725
0	1000	1.20000	3.79591	0.29159
0	1000	1.30000	3.81316	0.46803
0	1000	1.40000	3.82872	0.62433
0	1000	1.45000	3.83611	0.69628
0	1000	1.50000	3.84341	0.76530
0	1000	1.54000	3.84855	0.81728
0	1000	1.60000	3.85482	0.89291
0	1000	1.70000	3.86015	1.01260
0	1000	1.80000	3.85713	1.12389
0	1000	1.90000	3.84588	1.23260
0	1000	1.91000	3.84767	1.24875
0	1000	1.91500	3.85008	1.25887
0	1000	1.92000	3.85709	1.27678
0	1000	1.92500	3.87040	1.30607
0	1000	1.93000	3.88797	1.37559
0	1000	1.95000	3.87245	1.41807
0	1000	1.95400	3.86743	1.42494
0	1000	1.96200	3.84673	1.43204
0	1000	1.96600	3.83163	1.42992
0	1000	1.96800	3.81836	1.42292
0	1000	1.96900	3.80306	1.40808
0	1000	1.97000	3.79564	1.39787
0	1000	1.97400	3.76855	1.32206
0	1000	1.97600	3.74509	1.19045
0	1000	1.97800	3.72258	1.08958
0	1000	1.97900	3.71797	1.09934
0	1000	1.98100	3.71056	1.15725
0	1000	1.98200	3.70709	1.20857
0	1000	1.99000	3.69320	1.48019
0	1000	2.00000	3.67947	1.73567
0	1000	2.02000	3.65704	2.11526
0	1000	2.03000	3.61677	2.69923
0	2500	0.70000	3.64888	-0.83902
0	2500	0.75000	3.67183	-0.69615
0	2500	0.85000	3.71169	-0.43088
0	2500	0.90000	3.72873	-0.30623
0	2500	0.95000	3.74393	-0.18563
0	2500	1.00000	3.75735	-0.06825
0	2500	1.10000	3.77973	0.15955
0	2500	1.20000	3.79652	0.37132
0	2500	1.25000	3.80143	0.46383
0	2500	1.30000	3.80298	0.54658
0	2500	1.36000	3.79974	0.63472
0	2500	1.41000	3.79967	0.72635
0	2500	1.41300	3.80651	0.76339
0	2500	1.41600	3.81580	0.81974
0	2500	1.42000	3.81431	0.83524

Continued on next page

TABLE 1 – continued from previous page

ρ_χ (GeV cm^{-3})	*Age* (Myr)	$M(\mathrm{M}_\odot)$	$\log(T_{eff}$ / K)	$\log(L_\star$ / $\mathrm{L}_\odot$)
0	2500	1.43000	3.81240	0.85975
0	2500	1.44000	3.80895	0.88391
0	2500	1.45000	3.80463	0.90585
0	2500	1.46000	3.79809	0.92650
0	2500	1.46400	3.79489	0.93310
0	2500	1.46800	3.78899	0.93793
0	2500	1.47200	3.78720	0.94176
0	2500	1.47600	3.77708	0.93353
0	2500	1.48000	3.76533	0.90942
0	2500	1.48400	3.74951	0.85217
0	2500	1.48500	3.75394	0.87314
0	2500	1.48800	3.73419	0.78814
0	2500	1.49000	3.72322	0.75467
0	2500	1.49200	3.72011	0.75224
0	2500	1.49600	3.71147	0.77299
0	2500	1.50000	3.70672	0.82157
0	2500	1.51000	3.70153	0.93898
0	2500	1.52000	3.69624	1.09652
0	2500	1.53000	3.68671	1.33581
0	2500	1.53500	3.67794	1.51972
0	2500	1.53800	3.67202	1.63355
0	2500	1.53970	3.66811	1.70777
0	5000	0.70000	3.65207	-0.81780
0	5000	0.75000	3.67569	-0.66929
0	5000	0.85000	3.71673	-0.38839
0	5000	0.90000	3.73415	-0.25306
0	5000	0.95000	3.74950	-0.11874
0	5000	1.00000	3.76244	0.01398
0	5000	1.05000	3.77306	0.14705
0	5000	1.10000	3.78020	0.27460
0	5000	1.14000	3.78397	0.38615
0	5000	1.15000	3.78457	0.41565
0	5000	1.17000	3.78514	0.47905
0	5000	1.18000	3.78441	0.51244
0	5000	1.19000	3.78335	0.54390
0	5000	1.20000	3.78154	0.57640
0	5000	1.21000	3.77751	0.61223
0	5000	1.22000	3.77125	0.64143
0	5000	1.22400	3.76601	0.64974
0	5000	1.22800	3.75923	0.65024
0	5000	1.23200	3.74906	0.63586
0	5000	1.23300	3.74200	0.61838
0	5000	1.23400	3.74069	0.61596
0	5000	1.23500	3.74155	0.61948
0	5000	1.23600	3.72723	0.58247
0	5000	1.23700	3.72369	0.57655
0	5000	1.23900	3.71812	0.57240
0	5000	1.24000	3.71011	0.58288
0	5000	1.24600	3.70190	0.65929
0	5000	1.24800	3.70018	0.69494
0	5000	1.24900	3.69792	0.75628
0	5000	1.25000	3.69732	0.77741
0	5000	1.25500	3.69445	0.88494
0	5000	1.26000	3.68739	1.10785
0	5000	1.27000	3.65948	1.71237
0	5000	1.27100	3.65081	1.86220
0	10000	0.70000	3.65883	-0.77354
0	10000	0.75000	3.68387	-0.61118
0	10000	0.85000	3.72710	-0.28840
0	10000	0.90000	3.74406	-0.12341
0	10000	0.95000	3.75684	0.05096
0	10000	0.96000	3.75849	0.08575
0	10000	0.97000	3.75991	0.12365
0	10000	0.99000	3.76159	0.20510
0	10000	0.99600	3.76163	0.23140
0	10000	1.00300	3.76118	0.26305
0	10000	1.00800	3.76031	0.28752
0	10000	1.01200	3.75935	0.30657
0	10000	1.01800	3.75698	0.33548
0	10000	1.02200	3.75448	0.35441
0	10000	1.02700	3.74890	0.37717
0	10000	1.03000	3.74360	0.38685
0	10000	1.03200	3.73903	0.39007
0	10000	1.03400	3.73225	0.38940
0	10000	1.03500	3.72750	0.38722

Continued on next page

TABLE 1 – continued from previous page

ρ_χ (GeV cm^{-3})	*Age* (Myr)	$M(\mathrm{M}_\odot)$	$\log(T_{eff}$ / K)	$\log(L_\star$ / $\mathrm{L}_\odot$)
0	10000	1.03600	3.72339	0.38579
0	10000	1.03680	3.71901	0.38531
0	10000	1.03720	3.71672	0.38593
0	10000	1.03800	3.71246	0.38952
0	10000	1.03880	3.70827	0.39788
0	10000	1.04000	3.70379	0.41656
0	10000	1.04030	3.70263	0.42389
0	10000	1.04050	3.70193	0.42897
0	10000	1.04070	3.70126	0.43440
0	10000	1.04100	3.70031	0.44326
0	10000	1.04130	3.69943	0.45274
0	10000	1.04160	3.69878	0.46080
0	10000	1.04190	3.69793	0.47273
0	10000	1.04300	3.69567	0.51601
0	10000	1.04380	3.69436	0.55155
0	10000	1.04500	3.69276	0.61013
0	10000	1.05000	3.68530	0.92676
0	10000	1.05500	3.65768	1.59461
0	10000	1.05600	3.63176	2.03457
10^9	25	0.75000	3.65940	-0.77514
10^9	25	0.80000	3.67935	-0.64364
10^9	25	0.90000	3.71323	-0.40504
10^9	25	1.00000	3.74020	-0.19188
10^9	25	1.10000	3.76673	0.03980
10^9	25	1.20000	3.78723	0.22969
10^9	25	1.30000	3.80465	0.37837
10^9	25	1.40000	3.82367	0.53444
10^9	25	1.45000	3.83408	0.60678
10^9	25	1.50000	3.84579	0.67480
10^9	25	1.55000	3.85956	0.74008
10^9	25	1.60000	3.87333	0.80141
10^9	25	1.70000	3.89843	0.91551
10^9	25	1.80000	3.92057	1.02029
10^9	25	1.90000	3.94038	1.11764
10^9	25	2.00000	3.95837	1.20887
10^9	25	2.05000	3.96680	1.25246
10^9	25	2.20000	3.99024	1.37628
10^9	25	2.30000	4.00447	1.45354
10^9	25	2.50300	4.03062	1.59952
10^9	25	2.70000	4.05324	1.72939
10^9	25	2.90000	4.07398	1.85132
10^9	25	3.10000	4.09295	1.96473
10^9	25	3.20000	4.10184	2.01861
10^9	100	0.75000	3.64806	-0.78361
10^9	100	0.80000	3.67539	-0.63812
10^9	100	0.90000	3.70817	-0.41027
10^9	100	1.00000	3.73923	-0.18932
10^9	100	1.10000	3.76768	0.04934
10^9	100	1.20000	3.78884	0.23968
10^9	100	1.30000	3.80555	0.38429
10^9	100	1.40000	3.82488	0.54176
10^9	100	1.50000	3.84740	0.68206
10^9	100	1.55000	3.86078	0.74663
10^9	100	1.60000	3.87416	0.80796
10^9	100	1.70000	3.89848	0.92257
10^9	100	1.80000	3.91986	1.02830
10^9	100	1.85000	3.92962	1.07836
10^9	100	1.95000	3.94760	1.17383
10^9	100	2.00000	3.95586	1.21921
10^9	100	2.10000	3.97120	1.30657
10^9	100	2.20000	3.98528	1.38950
10^9	100	2.30000	3.99825	1.46867
10^9	100	2.40000	4.01033	1.54459
10^9	100	2.55000	4.02706	1.65298
10^9	100	2.70000	4.04232	1.75583
10^9	100	2.90000	4.06061	1.88549
10^9	100	3.10000	4.07678	2.00799
10^9	100	3.30000	4.09091	2.12462
10^9	100	3.50000	4.10297	2.23652

Continued on next page

TABLE 1 – continued from previous page

ρ_χ (GeV cm^{-3})	*Age* (Myr)	$M(\mathrm{M}_\odot)$	$\log(T_{eff}$ / K)	$\log(L_\star$ / $\mathrm{L}_\odot$)
10^9	250	0.70000	3.62785	-0.90881
10^9	250	0.75000	3.64613	-0.78529
10^9	250	0.80000	3.66922	-0.65203
10^9	250	0.85000	3.68911	-0.52894
10^9	250	0.90000	3.70751	-0.40976
10^9	250	0.95000	3.72422	-0.29562
10^9	250	1.00000	3.73964	-0.18478
10^9	250	1.10000	3.76808	0.05528
10^9	250	1.20000	3.78943	0.24738
10^9	250	1.30000	3.80616	0.39328
10^9	250	1.40000	3.82525	0.55156
10^9	250	1.50000	3.84766	0.69357
10^9	250	1.60000	3.87383	0.82152
10^9	250	1.70000	3.89678	0.93757
10^9	250	1.80000	3.91656	1.04530
10^9	250	1.90000	3.93334	1.14580
10^9	250	2.00000	3.94805	1.24091
10^9	250	2.10000	3.96105	1.33161
10^9	250	2.20000	3.97272	1.41878
10^9	250	2.30000	3.98325	1.50318
10^9	250	2.40000	3.99248	1.58492
10^9	250	2.50000	4.00055	1.66414
10^9	250	2.60000	4.00723	1.74164
10^9	250	2.70000	4.01235	1.81718
10^9	250	2.80000	4.01568	1.89125
10^9	250	2.90000	4.01648	1.96371
10^9	250	3.00000	4.01418	2.03443
10^9	250	3.10000	4.00774	2.10327
10^9	250	3.20000	4.00364	2.18023
10^9	250	3.22400	4.03716	2.24556
10^9	250	3.22500	4.04565	2.26296
10^9	250	3.22700	4.04611	2.27168
10^9	250	3.24000	4.03188	2.30772
10^9	250	3.24700	4.02709	2.31824
10^9	250	3.26000	4.00662	2.33630
10^9	250	3.26400	3.99822	2.33867
10^9	250	3.26800	3.97859	2.33592
10^9	250	3.27200	3.95230	2.32383
10^9	250	3.27300	3.91576	2.29236
10^9	250	3.27400	3.90395	2.28243
10^9	250	3.27500	3.87751	2.25651
10^9	250	3.27600	3.86864	2.24285
10^9	250	3.27700	3.83463	2.20543
10^9	250	3.27730	3.82712	2.19689
10^9	250	3.27740	3.82298	2.19149
10^9	250	3.27745	3.82002	2.18525
10^9	250	3.27747	3.82052	2.18883
10^9	250	3.27749	3.77211	2.10763
10^9	250	3.27750	3.77179	2.10691
10^9	250	3.27755	3.77195	2.10634
10^9	250	3.27760	3.76892	2.09917
10^9	250	3.27780	3.76524	2.09003
10^9	250	3.27800	3.75722	2.05817
10^9	250	3.27900	3.76627	2.09479
10^9	250	3.28000	3.74096	1.97505
10^9	250	3.28020	3.73469	1.93495
10^9	250	3.28040	3.73238	1.92099
10^9	250	3.28080	3.72446	1.87712
10^9	250	3.28085	3.72644	1.88832
10^9	250	3.28090	3.72762	1.89205
10^9	250	3.28095	3.72441	1.87706
10^9	250	3.28097	3.72408	1.87363
10^9	250	3.28098	3.71088	1.87058
10^9	250	3.28099	3.70322	1.91200
10^9	250	3.28100	3.70327	1.91151
10^9	250	3.28200	3.69780	1.96676
10^9	250	3.28250	3.68832	2.08389
10^9	500	0.75000	3.64408	-0.79070
10^9	500	0.80000	3.66957	-0.64842

Continued on next page

TABLE 1 – continued from previous page

ρ_χ (GeV cm^{-3})	*Age* (Myr)	$M(\mathrm{M}_\odot)$	$\log(T_{eff}$ / K)	$\log(L_\star$ / $\mathrm{L}_\odot$)
10^9	500	0.90000	3.70757	-0.40717
10^9	500	1.00000	3.74034	-0.17884
10^9	500	1.10000	3.76910	0.06393
10^9	500	1.20000	3.79009	0.25818
10^9	500	1.30000	3.80671	0.40618
10^9	500	1.40000	3.82572	0.56822
10^9	500	1.50000	3.84757	0.71313
10^9	500	1.59000	3.86913	0.83031
10^9	500	1.70000	3.89115	0.96164
10^9	500	1.80000	3.90685	1.07248
10^9	500	1.90000	3.91915	1.17711
10^9	500	2.00000	3.92890	1.27779
10^9	500	2.05000	3.93269	1.32681
10^9	500	2.10000	3.93572	1.37506
10^9	500	2.20000	3.93900	1.46899
10^9	500	2.30000	3.93758	1.55986
10^9	500	2.40000	3.92935	1.64569
10^9	500	2.45000	3.92343	1.68908
10^9	500	2.46000	3.92284	1.69862
10^9	500	2.48000	3.92464	1.72265
10^9	500	2.49000	3.93121	1.74291
10^9	500	2.49300	3.93461	1.75012
10^9	500	2.49700	3.94584	1.76993
10^9	500	2.49850	3.95222	1.78142
10^9	500	2.49900	3.95715	1.79112
10^9	500	2.49960	3.96773	1.81300
10^9	500	2.50300	3.96527	1.83684
10^9	500	2.50600	3.96201	1.84632
10^9	500	2.51000	3.95950	1.85424
10^9	500	2.52000	3.95287	1.87321
10^9	500	2.53000	3.94197	1.88995
10^9	500	2.54000	3.91884	1.89836
10^9	500	2.54200	3.90416	1.89429
10^9	500	2.54600	3.86379	1.86872
10^9	500	2.54700	3.85697	1.86313
10^9	500	2.54900	3.81757	1.82244
10^9	500	2.54930	3.80455	1.80574
10^9	500	2.54960	3.80038	1.79991
10^9	500	2.55000	3.76616	1.70926
10^9	500	2.55100	3.75226	1.63132
10^9	500	2.55150	3.75690	1.65548
10^9	500	2.55200	3.75174	1.62251
10^9	500	2.55250	3.74014	1.53703
10^9	500	2.55260	3.73943	1.53622
10^9	500	2.55280	3.73715	1.51841
10^9	500	2.55285	3.73741	1.52336
10^9	500	2.55290	3.72144	1.45710
10^9	500	2.55295	3.72082	1.45723
10^9	500	2.55300	3.72156	1.46155
10^9	500	2.55350	3.71900	1.45872
10^9	500	2.55400	3.71281	1.49296
10^9	500	2.55500	3.70704	1.55170
10^9	500	2.55600	3.70201	1.62113
10^9	500	2.56000	3.68100	1.95350
10^9	500	2.56100	3.67724	2.01236
10^9	500	2.56200	3.66962	2.12881
10^9	500	2.56300	3.66625	2.17883
10^9	500	2.56350	3.66608	2.18152
10^9	1000	0.75000	3.64863	-0.77614
10^9	1000	0.80000	3.66765	-0.65340
10^9	1000	0.85000	3.69086	-0.51828
10^9	1000	0.90000	3.70809	-0.40172
10^9	1000	0.95000	3.72571	-0.28306
10^9	1000	1.00000	3.74146	-0.16867
10^9	1000	1.05000	3.75528	-0.05891
10^9	1000	1.10000	3.77047	0.07985
10^9	1000	1.15000	3.78125	0.18185
10^9	1000	1.20000	3.79132	0.28015
10^9	1000	1.25000	3.79846	0.34292

Continued on next page

TABLE 1 – continued from previous page

ρ_χ (GeV cm^{-3})	*Age* (Myr)	$M(\mathrm{M}_\odot)$	$\log(T_{eff}$ / K)	$\log(L_\star$ / $\mathrm{L}_\odot$)
10^9	1000	1.30000	3.80798	0.43478
10^9	1000	1.36000	3.81870	0.53583
10^9	1000	1.40000	3.82578	0.60156
10^9	1000	1.45000	3.83472	0.67831
10^9	1000	1.50000	3.84384	0.75070
10^9	1000	1.55000	3.85216	0.81785
10^9	1000	1.60000	3.85892	0.88337
10^9	1000	1.65000	3.86407	0.94516
10^9	1000	1.70000	3.86683	1.00491
10^9	1000	1.75000	3.86835	1.06331
10^9	1000	1.80000	3.86693	1.11966
10^9	1000	1.85000	3.86274	1.17342
10^9	1000	1.90000	3.85571	1.22530
10^9	1000	1.93000	3.85144	1.25821
10^9	1000	1.94000	3.85155	1.27213
10^9	1000	1.95000	3.85502	1.29060
10^9	1000	1.96000	3.87631	1.33767
10^9	1000	1.97000	3.89319	1.41817
10^9	1000	1.98000	3.88974	1.44101
10^9	1000	1.99000	3.88288	1.46386
10^9	1000	2.00000	3.87156	1.48272
10^9	1000	2.00500	3.85922	1.48955
10^9	1000	2.00800	3.84669	1.48975
10^9	1000	2.01100	3.83247	1.48554
10^9	1000	2.01400	3.80006	1.46040
10^9	1000	2.01700	3.77624	1.40920
10^9	1000	2.01800	3.76002	1.33634
10^9	1000	2.02000	3.73630	1.18505
10^9	1000	2.02050	3.73211	1.16281
10^9	1000	2.02100	3.72376	1.13597
10^9	1000	2.02150	3.71762	1.14516
10^9	1000	2.02200	3.71595	1.15342
10^9	1000	2.02300	3.71265	1.17846
10^9	1000	2.02400	3.70511	1.28258
10^9	1000	2.02800	3.69387	1.49529
10^9	1000	2.03000	3.68954	1.57652
10^9	1000	2.04000	3.67028	1.91074
10^9	1000	2.05000	3.65965	2.08876
10^9	1000	2.06000	3.62073	2.65588
10^9	2500	0.75000	3.64424	-0.78350
10^9	2500	0.80000	3.66878	-0.64369
10^9	2500	0.85000	3.69109	-0.50990
10^9	2500	0.90000	3.71067	-0.38350
10^9	2500	0.95000	3.72878	-0.25901
10^9	2500	1.00000	3.74464	-0.13905
10^9	2500	1.05000	3.75891	-0.02038
10^9	2500	1.10000	3.77392	0.12937
10^9	2500	1.15000	3.78460	0.24225
10^9	2500	1.20000	3.79403	0.35057
10^9	2500	1.25000	3.79990	0.41950
10^9	2500	1.30000	3.80672	0.51870
10^9	2500	1.36000	3.80966	0.62345
10^9	2500	1.40000	3.80714	0.68143
10^9	2500	1.44000	3.80200	0.73701
10^9	2500	1.45000	3.80077	0.75093
10^9	2500	1.46000	3.80014	0.76998
10^9	2500	1.47000	3.80387	0.80321
10^9	2500	1.47400	3.80837	0.82857
10^9	2500	1.47500	3.82174	0.89839
10^9	2500	1.47800	3.82165	0.90921
10^9	2500	1.48000	3.82125	0.91408
10^9	2500	1.50000	3.81726	0.96577
10^9	2500	1.51000	3.81292	0.99287
10^9	2500	1.53000	3.79977	1.03847
10^9	2500	1.53400	3.79405	1.04669
10^9	2500	1.53800	3.78823	1.05125
10^9	2500	1.54200	3.77927	1.04842
10^9	2500	1.54600	3.76432	1.02028
10^9	2500	1.55000	3.74863	0.96063

Continued on next page

TABLE 1 – continued from previous page

ρ_χ (GeV cm^{-3})	*Age* (Myr)	$M(\mathrm{M}_\odot)$	$\log(T_{eff}$ / K)	$\log(L_\star$ / $\mathrm{L}_\odot$)
10^9	2500	1.55200	3.72995	0.87248
10^9	2500	1.55300	3.72165	0.85150
10^9	2500	1.55350	3.71679	0.85115
10^9	2500	1.55400	3.71266	0.86478
10^9	2500	1.55600	3.70693	0.91608
10^9	2500	1.55800	3.70279	0.98865
10^9	2500	1.56000	3.70049	1.04267
10^9	2500	1.57000	3.68788	1.34772
10^9	2500	1.58000	3.66395	1.80796
10^9	2500	1.58100	3.66014	1.87557
10^9	5000	0.75000	3.64640	-0.77180
10^9	5000	0.80000	3.67425	-0.61878
10^9	5000	0.85000	3.69490	-0.48554
10^9	5000	0.90000	3.71525	-0.35117
10^9	5000	0.95000	3.73403	-0.21566
10^9	5000	1.00000	3.75046	-0.08181
10^9	5000	1.05000	3.76474	0.05411
10^9	5000	1.10000	3.77823	0.22569
10^9	5000	1.15000	3.78537	0.35412
10^9	5000	1.17000	3.78721	0.40756
10^9	5000	1.20000	3.78911	0.47904
10^9	5000	1.22000	3.79055	0.55209
10^9	5000	1.23000	3.79010	0.58454
10^9	5000	1.25000	3.79241	0.62423
10^9	5000	1.27000	3.78795	0.69228
10^9	5000	1.27500	3.78626	0.71037
10^9	5000	1.28000	3.78342	0.73052
10^9	5000	1.28500	3.77986	0.75002
10^9	5000	1.29000	3.77557	0.76661
10^9	5000	1.29500	3.76825	0.77843
10^9	5000	1.30000	3.75508	0.77224
10^9	5000	1.30200	3.75176	0.76711
10^9	5000	1.30300	3.74258	0.74291
10^9	5000	1.30400	3.73698	0.72577
10^9	5000	1.30500	3.72483	0.69252
10^9	5000	1.30600	3.71911	0.68500
10^9	5000	1.30700	3.71121	0.69561
10^9	5000	1.30770	3.70509	0.73789
10^9	5000	1.30830	3.70498	0.74000
10^9	5000	1.30900	3.70290	0.76802
10^9	5000	1.31000	3.70110	0.80051
10^9	5000	1.31500	3.69144	1.06699
10^9	5000	1.32000	3.67088	1.52995
10^9	5000	1.32200	3.66317	1.68432
10^9	10000	0.75000	3.65292	-0.74005
10^9	10000	0.80000	3.67858	-0.58609
10^9	10000	0.85000	3.70306	-0.43126
10^9	10000	0.90000	3.72526	-0.27330
10^9	10000	0.95000	3.74416	-0.11285
10^9	10000	0.97000	3.75105	-0.04468
10^9	10000	1.00000	3.75934	0.06140
10^9	10000	1.02000	3.76377	0.13498
10^9	10000	1.04000	3.76530	0.20115
10^9	10000	1.05000	3.76880	0.25944
10^9	10000	1.06000	3.77067	0.30809
10^9	10000	1.07000	3.76783	0.39441
10^9	10000	1.08000	3.76446	0.45089
10^9	10000	1.08300	3.76259	0.46879
10^9	10000	1.09000	3.75423	0.50814
10^9	10000	1.09200	3.75034	0.51868
10^9	10000	1.09600	3.73617	0.52357
10^9	10000	1.09900	3.71296	0.51744
10^9	10000	1.09930	3.71123	0.52080
10^9	10000	1.09970	3.70776	0.53190
10^9	10000	1.10000	3.70365	0.55586
10^9	10000	1.10050	3.70349	0.55774
10^9	10000	1.10100	3.69885	0.61259
10^9	10000	1.10300	3.69213	0.79446
10^9	10000	1.10500	3.68442	1.04566

Continued on next page

TABLE 1 – continued from previous page

ρ_χ (GeV cm^{-3})	*Age* (Myr)	$M(\mathrm{M}_\odot)$	$\log(T_{eff}$ / K)	$\log(L_\star$ / $\mathrm{L}_\odot$)
10^9	10000	1.10550	3.68314	1.08039
10^9	10000	1.10600	3.67717	1.23010
10^{10}	25	0.80000	3.60171	-0.72426
10^{10}	25	0.90000	3.62789	-0.53664
10^{10}	25	1.00000	3.65060	-0.37636
10^{10}	25	1.10000	3.67594	-0.21872
10^{10}	25	1.20000	3.70175	-0.05352
10^{10}	25	1.30000	3.72801	0.12656
10^{10}	25	1.40000	3.75677	0.34375
10^{10}	25	1.45000	3.77470	0.47998
10^{10}	25	1.50000	3.79134	0.60358
10^{10}	25	1.55000	3.80644	0.70678
10^{10}	25	1.60000	3.82172	0.79405
10^{10}	25	1.65000	3.83954	0.87054
10^{10}	25	1.70000	3.85951	0.93735
10^{10}	25	1.74000	3.87459	0.98642
10^{10}	25	1.76000	3.88176	1.00993
10^{10}	25	1.80000	3.89513	1.05477
10^{10}	25	1.90000	3.92377	1.15625
10^{10}	25	2.00000	3.94699	1.24669
10^{10}	25	2.10000	3.96680	1.32970
10^{10}	25	2.20000	3.98423	1.40794
10^{10}	25	2.30000	3.99997	1.48214
10^{10}	25	2.40000	4.01437	1.55285
10^{10}	25	2.50000	4.02765	1.62046
10^{10}	25	2.60000	4.04003	1.68535
10^{10}	25	2.70000	4.05162	1.74769
10^{10}	25	2.80000	4.06255	1.80782
10^{10}	25	3.00000	4.08279	1.92198
10^{10}	25	3.10000	4.09219	1.97628
10^{10}	25	3.20000	4.10120	2.02890
10^{10}	100	0.70000	3.59342	-0.62850
10^{10}	100	0.80000	3.61265	-0.50389
10^{10}	100	0.90000	3.62725	-0.40982
10^{10}	100	1.00000	3.64231	-0.30581
10^{10}	100	1.10000	3.65872	-0.20290
10^{10}	100	1.20000	3.67634	-0.09159
10^{10}	100	1.30000	3.69853	0.03759
10^{10}	100	1.40000	3.73490	0.24217
10^{10}	100	1.45000	3.76230	0.41585
10^{10}	100	1.50000	3.78906	0.59608
10^{10}	100	1.55000	3.80725	0.71209
10^{10}	100	1.60000	3.82376	0.80198
10^{10}	100	1.65000	3.84275	0.87850
10^{10}	100	1.70000	3.86286	0.94459
10^{10}	100	1.76000	3.88460	1.01625
10^{10}	100	1.80000	3.89750	1.06027
10^{10}	100	1.90000	3.92475	1.16086
10^{10}	100	2.00000	3.94693	1.25173
10^{10}	100	2.10000	3.96564	1.33581
10^{10}	100	2.20000	3.98181	1.41497
10^{10}	100	2.30000	3.99615	1.49024
10^{10}	100	2.40000	4.00909	1.56242
10^{10}	100	2.50000	4.02099	1.63209
10^{10}	100	2.60000	4.03205	1.69954
10^{10}	100	2.70000	4.04239	1.76480
10^{10}	100	2.70200	4.04259	1.76607
10^{10}	100	2.80000	4.05207	1.82829
10^{10}	100	3.00000	4.06971	1.95027
10^{10}	100	3.10000	4.07771	2.00893
10^{10}	100	3.20000	4.08521	2.06651
10^{10}	100	3.30000	4.09217	2.12272
10^{10}	100	3.40000	4.09866	2.17810
10^{10}	100	3.50000	4.10458	2.23242
10^{10}	250	0.70000	3.59349	-0.62775
10^{10}	250	0.80000	3.61265	-0.50389
10^{10}	250	0.90000	3.62766	-0.40301
10^{10}	250	1.00000	3.64230	-0.30329

Continued on next page

TABLE 1 – continued from previous page

ρ_χ (GeV cm^{-3})	Age (Myr)	$M(\mathrm{M}_\odot)$	$\log(T_{eff}$ / K)	$\log(L_\star$ / $\mathrm{L}_\odot$)
10^{10}	250	1.10000	3.65798	-0.19969
10^{10}	250	1.20000	3.67556	-0.09093
10^{10}	250	1.30000	3.69671	0.03406
10^{10}	250	1.40000	3.73128	0.22720
10^{10}	250	1.44000	3.75889	0.39117
10^{10}	250	1.53000	3.80126	0.67555
10^{10}	250	1.55000	3.80817	0.71798
10^{10}	250	1.60000	3.82542	0.80970
10^{10}	250	1.65000	3.84492	0.88633
10^{10}	250	1.70000	3.86508	0.95286
10^{10}	250	1.80000	3.89902	1.07001
10^{10}	250	1.90000	3.92480	1.17147
10^{10}	250	2.00000	3.94476	1.26280
10^{10}	250	2.11000	3.96228	1.35670
10^{10}	250	2.20000	3.97481	1.43071
10^{10}	250	2.30000	3.98578	1.50889
10^{10}	250	2.40000	3.99598	1.58609
10^{10}	250	2.50000	4.00488	1.66125
10^{10}	250	2.60000	4.01246	1.73526
10^{10}	250	2.70000	4.01859	1.80770
10^{10}	250	2.80000	4.02310	1.87882
10^{10}	250	3.00000	4.02552	2.01842
10^{10}	250	3.10000	4.02190	2.08620
10^{10}	250	3.20000	4.01430	2.15322
10^{10}	250	3.22000	4.01277	2.16722
10^{10}	250	3.24000	4.01174	2.18256
10^{10}	250	3.26000	4.01327	2.20081
10^{10}	250	3.28000	4.02670	2.23334
10^{10}	250	3.28500	4.04408	2.26151
10^{10}	250	3.29000	4.05639	2.29390
10^{10}	250	3.29500	4.05395	2.30856
10^{10}	250	3.30000	4.05357	2.31636
10^{10}	250	3.32000	4.04968	2.34698
10^{10}	250	3.33000	4.04627	2.36266
10^{10}	250	3.34000	4.04091	2.37787
10^{10}	250	3.35000	4.03370	2.39302
10^{10}	250	3.36000	4.01745	2.40485
10^{10}	250	3.37000	3.98897	2.40714
10^{10}	250	3.37200	3.95120	2.38532
10^{10}	250	3.37300	3.96704	2.39705
10^{10}	250	3.37350	3.92038	2.35792
10^{10}	250	3.37400	3.89185	2.32240
10^{10}	250	3.37500	3.87884	2.31104
10^{10}	250	3.37600	3.87480	2.30377
10^{10}	250	3.37610	3.82323	2.23956
10^{10}	250	3.37625	3.76925	2.14724
10^{10}	250	3.37630	3.75533	2.09758
10^{10}	250	3.37650	3.75340	2.08848
10^{10}	250	3.37800	3.74435	2.04126
10^{10}	250	3.37890	3.72552	1.92500
10^{10}	250	3.37900	3.71631	1.89722
10^{10}	250	3.37940	3.70380	1.94489
10^{10}	250	3.37970	3.69641	2.01061
10^{10}	250	3.38000	3.69639	2.01106
10^{10}	250	3.38050	3.68514	2.15606
10^{10}	250	3.38100	3.66782	2.39365
10^{10}	500	0.70000	3.59342	-0.62850
10^{10}	500	0.80000	3.61265	-0.50389
10^{10}	500	0.90000	3.62767	-0.40301
10^{10}	500	1.00000	3.64230	-0.30251
10^{10}	500	1.10000	3.65819	-0.20023
10^{10}	500	1.20000	3.67554	-0.09088
10^{10}	500	1.30000	3.69647	0.03344
10^{10}	500	1.40000	3.73118	0.22720
10^{10}	500	1.44000	3.75827	0.38808
10^{10}	500	1.53000	3.80224	0.68268
10^{10}	500	1.55000	3.80995	0.72853
10^{10}	500	1.60000	3.82760	0.82057
10^{10}	500	1.65000	3.84768	0.89791

Continued on next page

TABLE 1 – continued from previous page

ρ_χ (GeV cm^{-3})	*Age* (Myr)	$M(\mathrm{M}_\odot)$	$\log(T_{eff}$ / K)	$\log(L_\star$ / $\mathrm{L}_\odot$)
10^{10}	500	1.70000	3.86796	0.96601
10^{10}	500	1.76000	3.88850	1.03930
10^{10}	500	1.80000	3.90008	1.08457
10^{10}	500	1.90000	3.92217	1.18698
10^{10}	500	2.00000	3.93750	1.28114
10^{10}	500	2.10000	3.94795	1.37030
10^{10}	500	2.15000	3.95196	1.41438
10^{10}	500	2.20000	3.95509	1.45762
10^{10}	500	2.30000	3.95728	1.54300
10^{10}	500	2.40000	3.95542	1.62688
10^{10}	500	2.50000	3.94693	1.70742
10^{10}	500	2.55000	3.94184	1.75045
10^{10}	500	2.55600	3.94203	1.75654
10^{10}	500	2.55700	3.94212	1.75765
10^{10}	500	2.55800	3.94217	1.75880
10^{10}	500	2.55900	3.94228	1.75997
10^{10}	500	2.60000	3.99163	1.88475
10^{10}	500	2.62000	3.99297	1.92062
10^{10}	500	2.64000	3.99075	1.95728
10^{10}	500	2.66000	3.98326	1.99550
10^{10}	500	2.68000	3.96681	2.03021
10^{10}	500	2.68200	3.95995	2.03320
10^{10}	500	2.68600	3.95410	2.03834
10^{10}	500	2.68800	3.94773	2.04005
10^{10}	500	2.69200	3.92822	2.03882
10^{10}	500	2.69400	3.89373	2.01971
10^{10}	500	2.69420	3.89459	2.01915
10^{10}	500	2.69440	3.89070	2.01627
10^{10}	500	2.69460	3.89580	2.02186
10^{10}	500	2.69480	3.86146	1.98866
10^{10}	500	2.69500	3.86910	1.99730
10^{10}	500	2.69520	3.85675	1.98359
10^{10}	500	2.69540	3.87282	2.00053
10^{10}	500	2.69560	3.87244	2.00054
10^{10}	500	2.69580	3.83047	1.95416
10^{10}	500	2.69630	3.84622	1.97231
10^{10}	500	2.69660	3.78873	1.89355
10^{10}	500	2.69690	3.79320	1.90246
10^{10}	500	2.69710	3.76255	1.81118
10^{10}	500	2.69730	3.75139	1.74539
10^{10}	500	2.69750	3.74936	1.72820
10^{10}	500	2.69780	3.74743	1.72034
10^{10}	500	2.69795	3.73908	1.65063
10^{10}	500	2.69800	3.72122	1.54824
10^{10}	500	2.69860	3.71297	1.57353
10^{10}	500	2.69880	3.69589	1.78031
10^{10}	500	2.70000	3.68929	1.88306
10^{10}	500	2.70050	3.69252	1.83360
10^{10}	500	2.70070	3.68060	2.01429
10^{10}	1000	0.70000	3.59343	-0.62835
10^{10}	1000	0.80000	3.61265	-0.50388
10^{10}	1000	0.90000	3.62771	-0.40237
10^{10}	1000	1.00000	3.64227	-0.30241
10^{10}	1000	1.10000	3.65805	-0.19957
10^{10}	1000	1.20000	3.67568	-0.09093
10^{10}	1000	1.30000	3.69727	0.03518
10^{10}	1000	1.40000	3.73102	0.22653
10^{10}	1000	1.44000	3.75889	0.39277
10^{10}	1000	1.53000	3.80564	0.70306
10^{10}	1000	1.60000	3.83200	0.84284
10^{10}	1000	1.65000	3.85341	0.92307
10^{10}	1000	1.70000	3.87285	0.99406
10^{10}	1000	1.76000	3.88904	1.06749
10^{10}	1000	1.80000	3.89652	1.11273
10^{10}	1000	1.83000	3.90033	1.14480
10^{10}	1000	1.87000	3.90370	1.18600
10^{10}	1000	1.90000	3.90493	1.21566
10^{10}	1000	1.95000	3.90401	1.26376
10^{10}	1000	2.00000	3.90141	1.31448

Continued on next page

TABLE 1 – continued from previous page

ρ_χ (GeV cm^{-3})	*Age* (Myr)	$M(\mathrm{M}_\odot)$	$\log(T_{eff}$ / K)	$\log(L_\star$ / $\mathrm{L}_\odot$)
10^{10}	1000	2.05000	3.89407	1.36077
10^{10}	1000	2.06000	3.89241	1.37057
10^{10}	1000	2.07000	3.88761	1.37607
10^{10}	1000	2.08000	3.88835	1.38831
10^{10}	1000	2.09000	3.89412	1.41124
10^{10}	1000	2.11000	3.93148	1.48036
10^{10}	1000	2.12000	3.93149	1.49956
10^{10}	1000	2.12200	3.92995	1.54880
10^{10}	1000	2.16000	3.91064	1.62459
10^{10}	1000	2.16200	3.90691	1.62914
10^{10}	1000	2.16400	3.90554	1.63129
10^{10}	1000	2.16800	3.89927	1.63903
10^{10}	1000	2.17000	3.89056	1.64023
10^{10}	1000	2.17200	3.88933	1.64312
10^{10}	1000	2.17400	3.88375	1.64434
10^{10}	1000	2.17800	3.85624	1.63663
10^{10}	1000	2.17900	3.84939	1.63333
10^{10}	1000	2.18000	3.80882	1.59958
10^{10}	1000	2.18050	3.79955	1.58839
10^{10}	1000	2.18400	3.76397	1.48527
10^{10}	1000	2.18470	3.75255	1.42385
10^{10}	1000	2.18500	3.74623	1.37775
10^{10}	1000	2.18600	3.72835	1.26181
10^{10}	1000	2.18650	3.72407	1.24779
10^{10}	1000	2.18720	3.71856	1.25013
10^{10}	1000	2.18800	3.71212	1.28788
10^{10}	1000	2.19000	3.69462	1.56416
10^{10}	1000	2.19400	3.69228	1.60791
10^{10}	1000	2.19600	3.68734	1.69522
10^{10}	1000	2.20000	3.67855	1.84529
10^{10}	1000	2.21000	3.65633	2.19809
10^{10}	2500	0.70000	3.59349	-0.62780
10^{10}	2500	0.80000	3.61265	-0.50388
10^{10}	2500	0.90000	3.62767	-0.40301
10^{10}	2500	1.00000	3.64237	-0.30378
10^{10}	2500	1.10000	3.65825	-0.19978
10^{10}	2500	1.35000	3.70932	0.10914
10^{10}	2500	1.40000	3.73128	0.22828
10^{10}	2500	1.44000	3.75879	0.39584
10^{10}	2500	1.53000	3.81410	0.75816
10^{10}	2500	1.57000	3.83305	0.85851
10^{10}	2500	1.60000	3.84564	0.91821
10^{10}	2500	1.63000	3.85266	0.96669
10^{10}	2500	1.66000	3.85215	1.00609
10^{10}	2500	1.70000	3.84199	1.05047
10^{10}	2500	1.72000	3.83612	1.07915
10^{10}	2500	1.72100	3.85743	1.11808
10^{10}	2500	1.72200	3.86014	1.12466
10^{10}	2500	1.72400	3.87311	1.16259
10^{10}	2500	1.72800	3.87269	1.17369
10^{10}	2500	1.73200	3.87128	1.18566
10^{10}	2500	1.73600	3.87105	1.19157
10^{10}	2500	1.74000	3.87041	1.19929
10^{10}	2500	1.75000	3.86430	1.23096
10^{10}	2500	1.76000	3.86125	1.25416
10^{10}	2500	1.76300	3.85553	1.27278
10^{10}	2500	1.76900	3.85413	1.28327
10^{10}	2500	1.77200	3.85151	1.29184
10^{10}	2500	1.77500	3.84768	1.30132
10^{10}	2500	1.78100	3.83483	1.32116
10^{10}	2500	1.78400	3.82214	1.33031
10^{10}	2500	1.78700	3.81245	1.33483
10^{10}	2500	1.78850	3.80299	1.33387
10^{10}	2500	1.79000	3.78996	1.32675
10^{10}	2500	1.79200	3.77997	1.31361
10^{10}	2500	1.79300	3.76226	1.26238
10^{10}	2500	1.79450	3.75258	1.21969
10^{10}	2500	1.79550	3.73794	1.13340
10^{10}	2500	1.79560	3.73550	1.11770

Continued on next page

TABLE 1 – continued from previous page

ρ_χ (GeV cm^{-3})	*Age* (Myr)	$M(\mathrm{M}_\odot)$	$\log(T_{eff}$ / K)	$\log(L_\star$ / $\mathrm{L}_\odot$)
10^{10}	2500	1.79580	3.72151	1.05788
10^{10}	2500	1.79800	3.70862	1.11460
10^{10}	2500	1.80210	3.68846	1.49512
10^{10}	2500	1.80230	3.68561	1.54939
10^{10}	5000	0.70000	3.59343	-0.62848
10^{10}	5000	0.80000	3.61266	-0.50388
10^{10}	5000	0.90000	3.62768	-0.40294
10^{10}	5000	1.00000	3.64232	-0.30238
10^{10}	5000	1.10000	3.65825	-0.19996
10^{10}	5000	1.35000	3.71131	0.11569
10^{10}	5000	1.40000	3.73269	0.23555
10^{10}	5000	1.42000	3.74773	0.32335
10^{10}	5000	1.44000	3.75940	0.40507
10^{10}	5000	1.52500	3.82673	0.86081
10^{10}	5000	1.52900	3.82723	0.87224
10^{10}	5000	1.53000	3.82739	0.87449
10^{10}	5000	1.53200	3.82716	0.87939
10^{10}	5000	1.55000	3.82059	0.91006
10^{10}	5000	1.55400	3.81926	0.91844
10^{10}	5000	1.55500	3.81942	0.92292
10^{10}	5000	1.55600	3.82012	0.92808
10^{10}	5000	1.55700	3.82209	0.93831
10^{10}	5000	1.55800	3.82537	0.95100
10^{10}	5000	1.56000	3.83293	0.98387
10^{10}	5000	1.57000	3.82934	1.02482
10^{10}	5000	1.57400	3.82722	1.04105
10^{10}	5000	1.57800	3.82450	1.06319
10^{10}	5000	1.58200	3.82054	1.08576
10^{10}	5000	1.58600	3.81474	1.10958
10^{10}	5000	1.59000	3.80618	1.13377
10^{10}	5000	1.59200	3.80030	1.14496
10^{10}	5000	1.59400	3.79237	1.15433
10^{10}	5000	1.59600	3.78150	1.15645
10^{10}	5000	1.59700	3.77129	1.14679
10^{10}	5000	1.59800	3.76298	1.12934
10^{10}	5000	1.59850	3.75192	1.09169
10^{10}	5000	1.59900	3.74191	1.04429
10^{10}	5000	1.59930	3.73466	1.00691
10^{10}	5000	1.59970	3.73375	1.00286
10^{10}	5000	1.60000	3.72418	0.96280
10^{10}	5000	1.60020	3.71859	0.95378
10^{10}	5000	1.60040	3.70956	0.98761
10^{10}	5000	1.60060	3.70970	0.98616
10^{10}	5000	1.60070	3.70557	1.03330
10^{10}	5000	1.60100	3.70588	1.02912
10^{10}	5000	1.60200	3.69679	1.20695
10^{10}	5000	1.60300	3.68802	1.39689
10^{10}	5000	1.60400	3.66942	1.74128
10^{10}	5000	1.60500	3.65370	2.00792
10^{10}	5000	1.60600	3.64008	2.21617
10^{10}	10000	0.70000	3.59344	-0.62847
10^{10}	10000	0.80000	3.61267	-0.50388
10^{10}	10000	0.90000	3.62769	-0.40299
10^{10}	10000	1.30000	3.69722	0.03529
10^{10}	10000	1.40000	3.73533	0.24953
10^{10}	10000	1.41000	3.74352	0.29694
10^{10}	10000	1.46500	3.80456	0.70287
10^{10}	10000	1.48000	3.81716	0.82561
10^{10}	10000	1.48200	3.81629	0.84311
10^{10}	10398[1]	1.48200	3.81542	0.86725
10^{10}	11050[1]	1.48200	3.81191	0.92592
10^{10}	11480[1]	1.48200	3.80361	0.98288
10^{10}	11531[1]	1.48200	3.80181	0.99086
10^{10}	11764[1]	1.48200	3.78869	1.02901
10^{10}	11859[1]	1.48200	3.77838	1.04011
10^{10}	11886[1]	1.48200	3.77429	1.04049

Continued on next page

[1] In the case of $\rho_\chi = 10^{10}$ GeV cm^{-3}, the post-MS segment of the 10 Gyr isochrone is a conservative estimation (a lower limit on luminosity) of the true isochrone. It corresponds to the evolutionary track of a star of 1.482 $\mathrm{M}_\odot$.

TABLE 1 – continued from previous page

ρ_χ (GeV cm^{-3})	Age (Myr)	$M(\mathrm{M}_\odot)$	$\log(T_{eff}$ / K)	$\log(L_\star$ / $\mathrm{L}_\odot$)
10^{10}	11911[1]	1.48200	3.76976	1.03835
10^{10}	11953[1]	1.48200	3.75900	1.02202
10^{10}	11989[1]	1.48200	3.74529	0.97853
10^{10}	12011[1]	1.48200	3.73269	0.92437
10^{10}	12023[1]	1.48200	3.72535	0.89746
10^{10}	12030[1]	1.48200	3.72109	0.88802
10^{10}	12043[1]	1.48200	3.71376	0.89170
10^{10}	12055[1]	1.48200	3.70812	0.92433
10^{10}	12063[1]	1.48200	3.70488	0.96159
10^{10}	12073[1]	1.48200	3.70197	1.00946
10^{10}	12091[1]	1.48200	3.69698	1.11706
10^{10}	12101[1]	1.48200	3.69396	1.18796
10^{10}	12115[1]	1.48200	3.68955	1.28798
10^{10}	12125[1]	1.48200	3.68606	1.36247
10^{10}	12135[1]	1.48200	3.68178	1.44963
10^{10}	12146[1]	1.48200	3.67543	1.56985
10^{10}	12157[1]	1.48200	3.66829	1.69748
10^{10}	12161[1]	1.48200	3.66535	1.74837
10^{10}	12173[1]	1.48200	3.66014	1.84078
10^{10}	12184[1]	1.48200	3.65567	1.91832
10^{10}	12189[1]	1.48200	3.64898	2.02439